Optical Clock Distribution in Supercomputers using Polyimide-based Waveguides

Bipin Bihari*[a], Jianhua Gan[a], Linghui Wu[a], Yujie Liu[a], Suning Tang[b] and Ray T. Chen[a]

[a]Microelectronics Research Center, University of Texas at Austin, Austin, TX 78758

[b]Radiant Research, Inc., 3006 Longhorn Blvd., Suite 105, Austin, TX 78758

ABSTRACT

Guided-wave optics is a promising way to deliver high-speed clock-signal in supercomputer with minimized clock-skew. Si-CMOS compatible polymer-based waveguides for optoelectronic interconnects and packaging have been fabricated and characterized. A 1-to-48 fanout optoelectronic interconnection layer (OIL) structure based on Ultradel 9120/9020 for the high-speed massive clock signal distribution for a Cray T-90 supercomputer board has been constructed. The OIL employs multimode polymeric channel waveguides in conjunction with surface-normal waveguide output coupler and 1-to-2 splitters. Surface-normal couplers can couple the optical clock signals into and out from the H-tree polyimide waveguides surface-normally, which facilitates the integration of photodetectors to convert optical-signal to electrical-signal. A 45-degree surface-normal coupler has been integrated at the each output end. The measured output coupling efficiency is nearly 100%. The output profile from 45-degree surface-normal coupler were calculated using Fresnel approximation. The theoretical result is in good agreement with experimental result. A total insertion loss of 7.98 dB at 850 nm was measured experimentally.

Keywords: guided-wave optics, clock skew, surface-normal coupler, H-tree.

1. INTRODUCTION

The clock frequency is an important parameter determining performance of high-speed computing environments. State-of-the-art VLSI circuits are capable of operating and generating ultra-high clock rates (> 1 GHz). However, clock signal distribution systems based on electrical interconnect technologies fail to keep up with the cycle times and pulse widths needed to synchronize the operation of logic devices over long distances[1-3]. This timing bottleneck is a consequence of the variations in the transmission line propagation losses and dispersion, different packaging environments, and impedance discontinuities at the interfaces of the chips and boards. Further, capacitive loading, switching noise and signal cross-talk alter the clock signal waveform and become critical at high clock rates and large system lengths. These bottlenecks manifest themselves as clock skew and timing jitter in synchronous clock signal distribution systems. Guided-wave optical interconnects show great potentials to overcome these bottlenecks. For example, the latest T-90 microprocessor machines from Cray Research Inc. has up to 36 processor-boards with a system clock speed of 500 MHz. All the boards in this system are synchronized to a central clock using an optical clock signal distribution system utilizing a high power semiconductor laser operating in conjunction with a single-mode optical fibers at 1.3 μm. Within the board the clock signal distribution is still all electrical which puts a limitation on further improvements in the overall system speed. It is extremely difficult to obtain high-speed (>500 MHz), synchronous intra-board clock distribution using electrical interconnections due to large fanouts (48) and long interconnection lengths (> 15 cm)[1-5]. A fanout chip is required to provide mass intra-board electrical fanout. A synchronous global clock signal distribution at board level is highly desirable to simplify the architecture and to enable higher speed performance. High-speed, large-area massive fanout optoelectronic interconnects may overcome many of the problems associated with electrical interconnects in this interconnection scenario[1-9].

We have developed a guided-wave optoelectronic interconnect network for optical clock signal distribution in board-level multi-processor systems as shown in Fig.1(a). A H-tree waveguide structure has been designed and fabricated to provide equalized path lengths in order to minimize the clock skew problems. For comparison, the electrical fanout network currently employed by Cray Research is shown in Fig. 1(b) which shows the existing 500 MHz 1-to-48 electrical clock signal distribution realized in one of the 52 vertical integration layers within the Cray T-90 supercomputer board.

Part of the SPIE Conference on Optoelectronic Interconnects VI
San Jose, California • January 1999
SPIE Vol. 3632 • 0277-786X/99/$10.00

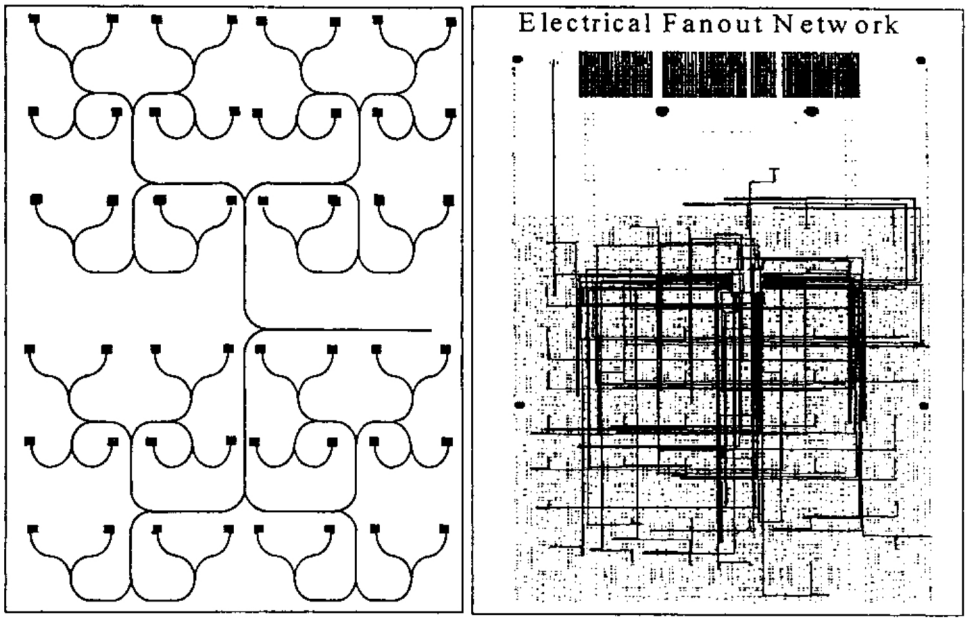

(b)

Fig.1 Schematic diagrams of massive clock signal distribution networks using (a) an optical waveguide H-tree and (b) an electrical transmission line network.

1. DESIGN AND FABRICATION OF H-TREE WAVEGUIDE

The guided-wave optoelectronic interconnect network under development is based on polymeric 1-to-48 fanout channel waveguides in conjunction with waveguide output couplers and fast photo-detectors. This network will be inserted into the Cray supercomputer boards as an additional interconnection layer along with the electrical interconnection layers. The Cray T-90 supercomputer board consists of 52 vertical electrical interconnection layers with the board size of 14.48 x 26.67 cm^2. In order to implement an additional optoelectronic interconnection layer (OIL), Si-CMOS process compatibility and planarization of the OIL are the two major concerns that need to be addressed. These two issues could be effectively handled by application of polyimide-based waveguide structures. Our approach utilizes low-loss polyimides for optical channel waveguides which are Si-CMOS process compatible and all associated components including waveguides, waveguide output couplers and waveguide splitters can be easily planarized.

The optical components required for constructing an H-tree system such as the one shown in Fig. 1(a) include low loss polymer-based channel waveguides, waveguide output couplers, and 3 dB 1-to-2 splitter waveguides. The basic design goals include:

1: **Minimizing the clock skew**

2: **Low waveguide propagation loss**

3: **Low 1-to-2 splitting and bending loss**

4: **Low input and output coupling loss**

5: **Large fanout and uniformity**

1.1 Materials

To ensure the desired electrical and mechanical properties imposed by the Cray supercomputer board, and to meet the required optical properties for the low-loss waveguide formation, Ultra-9000 series photosensitive polyimides (Amoco Chemicals)[10] are used for the waveguide fabrication. Polyimides are widely used in silicon CMOS processing. They are

thermally stable. For waveguide applications, the polyimides should have low optical loss and good thermal stability. We have used Ultradel 9120D to fabricate H-tree waveguide, a 1-to-48 fanout structure with equivalent optical paths. Ultradel-9120D is a negative-acting, photosensitive polyimide. At the wavelength of 1.310μm, the refractive indices are 1.5364 and 1.5073 for TE and TM waves, respectively. The optical losses of this material are 1.04dB/cm at 633nm, 0.13dB/cm at 830nm, 0.09dB/cm at 1064nm, 0.34dB/cm at 1300nm and 1.21dB/cm at 1550nm. The glass transition temperature and the coefficient of thermal expansion are 390 °C and 27ppm/°C @ 300 °C, respectively. The moisture uptake is very low (~ 3% at 100% relative humidity). Polyimides with lower refractive indices are also available for cladding and buffer coatings. Fully cross-linked polyimides have excellent thermal stability (Tg = 400 °C) and optical transparency. The high glass transition temperature(Tg) is critical for the polymer to survive wire-bonding and metal deposition process, which makes it compatible with CMOS processing. Ultra-9000 series photosensitive polyimides are transparent in the visible and near infrared regions, which allows us to employ VCSELs, having output wavelength around 850 nm, and employ silicon-based photodetectors. The photosensitivity of these polyimides also enables us to fabricate the waveguide using conventional photolithography.

1.2 Splitter Design

To achieve the required 1-to-48 fanout , we have used a 6-stage 90° bend 1-to-2 splitter. Fig. 2 shows the diagrams of 90° bend 1-to-2 splitter. The splitter includes a 3 mm-long tapered waveguide and two curved waveguides with radius of curvature of 3mm. The tapered waveguides have a width of 50 μm at one end and 100 μm at the other end. Compared to the conventional Y-branch design[11] ,We have shown experimentally that this structure can effectively reduce the splitting loss from >2dB to 0.4 dB per splitter.

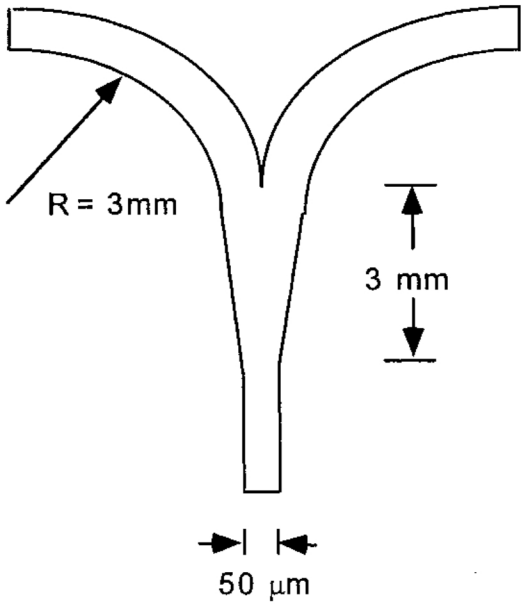

Fig. 2 Schematic diagram of 1-to-2 y-branch. The waveguide have width of 50 μm.

To select the bending curvature, we need a minimized curvature in order to reduce the area of the splitter. On the other hand, to minimize the bending loss a large curvature is prefered. The curvature of the splitter in our H-tree design is 3 mm. The width of waveguide is 50 μm. The bending loss can be estimated as[12]:

$$\frac{2}{\pi}\frac{1}{\sqrt{100\Delta}}10^{2.29-2.17R_n-0.58R_n^2}(\mathrm{dB/rad})$$

with $\Delta = \Delta N / Nb$ and $R_n = (N_b R / \lambda)\Delta^{\frac{3}{2}} * 1.137^{\Delta - 0.01}$

where ΔN is the refractive index difference of waveguide and buffer, Nb is the refractive index of substrate and R is the radius of the waveguide curvature. With ΔN equal to 0.07 and R equal to 3mm, theoretically, the bending loss is negligible($< 10^{-10}$ dB/rad).

1.3 Waveguide Fabrication and Characterization

We have constructed a 1-to-48 fanout H-tree waveguide structure using polyimide planarization and photolithography. A silicon wafer with 2μm thick silicon dioxide is used as substrate. Silicon dioxide layer acts as buffer layer. As an alternative, other low index polyimide can also be used as cladding and buffer layers. About 10-μm-thick polyimide 9120D is spin-coated on the clean substrate. H-tree structure is patterned to the polyimide layer using UV photolithography. The preparation and photolithography of 9120D film are briefly described here. Five milliliter of filtered (0.2μm) Ultradel A600 adhesion promoter was dispensed on a clean substrate, and spun for five-second @ 500 RPM followed by 30-second spin @ 4000 RPM. Residual solvent was removed by baking it @ 100°C for 60 seconds. Next, 5 ml of 9120D was applied and spun for 30-second @ 500 RPM followed by a 60-second-spin at the spin speed determined by targeted film-thickness (~ 1500 RPM for 10 μm thick film). The 9120D coating was baked for 3 minutes on a 100°C hotplate. At this stage the coating is ready for imaging and development. A typical exposure dosage required is approximately 300-900mJ/cm^2 with broadband ultraviolet (UV) light source. Post-exposure bake at 175°C for 30 minutes in a nitrogen-purged oven was used to improve fine feature resolution. After post-exposure bake the 9120D film was developed using spray development method and finally baked at 300°C for 30-60 minutes in a nitrogen-purged oven.

Fig. 3 shows microscope pictures of the H-tree components fabricated using above procedure. The 3dB 1-to-2 splitter structure is shown in (a). Fig. 3(b) shows the fanout end of the waveguide. Fig. 3(c) and (d) shows the tapered portion and curved portion of the waveguides.

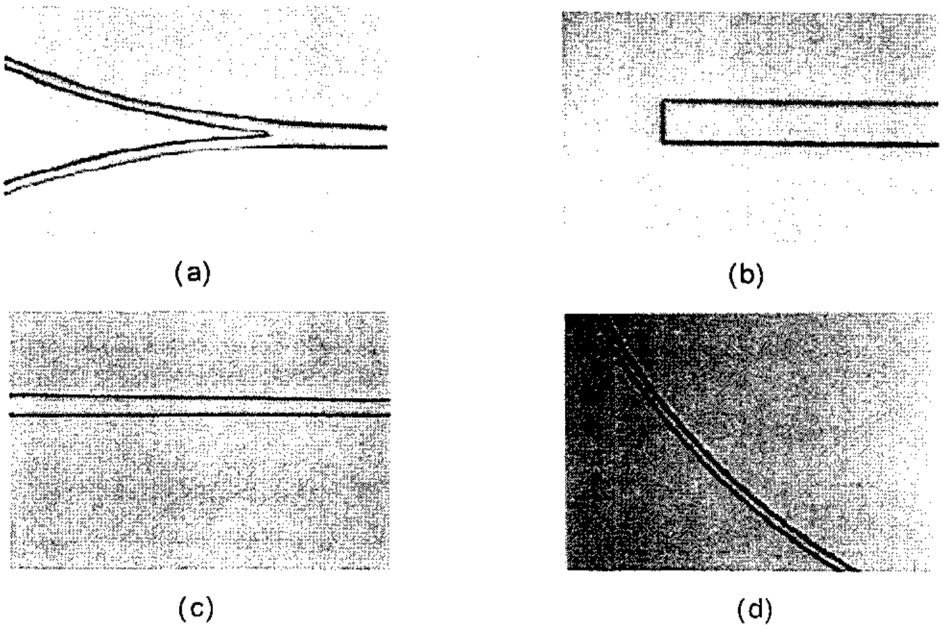

Fig. 3. Microscope pictures of the H-tree structure. (a) is the picture of splitter. (b) is the picture of the end of the H-tree. (c) and (d) show the tapered and curved waveguides. All the waveguides have width of 50 μm except the tapered regions.

Fig. 4 shows a photograph of the waveguide H-tree system showing the 633 nm He-Ne laser light coupled into the input end of the OIL. Fairly uniform light distribution to the 48 fanout can be clearly seen in Fig. 4. However, It should be noted that this photograph was taken at a very small angle with respect to the substrate surface. Nothing was visible when this sample was viewed from perpendicular direction. Our goal was to have all the output coupled out surface-normally to facilitate convenient integration of the photodetectors.

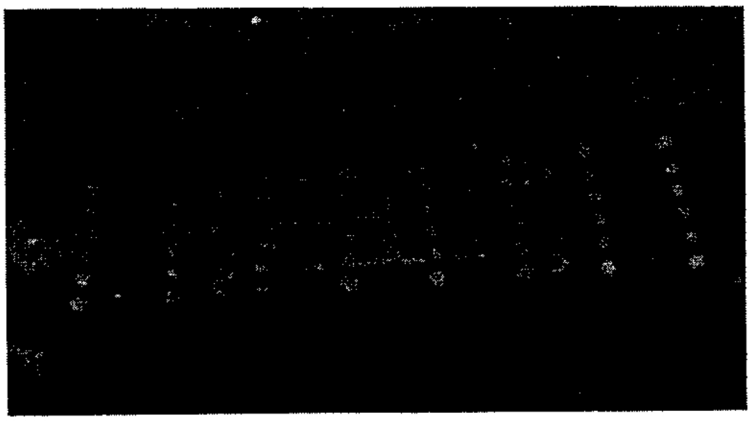

Fig. 4 Photograph of the 1-to-48 fanout H-tree on Si substrate using Ultradel 9120 polyimide. A He-Ne laser beam at λ=633 nm was butt-coupled into the input end.

2. WAVEGUIDE COUPLERS

Any guided-wave optoelectronic interconnection configuration involves the coupling of the light signal from the source (e.g. VCSEL) to waveguide and the coupling of it from the waveguide to photo-detectors. Thus surface-normal micro-coupler is a key component in the planar integrated optical systems. Surface-normal micro-couplers facilitate the integration of vertical cavity surface-emitting lasers (VCSEL) and photo diodes with optical waveguides. Employment of conventional coupling techniques utilizing prisms, lenses is costly, bulky and very inconvenient from the packaging point of view and often put restriction on planarization. The waveguide grating or waveguide mirror based coupler can overcome above problems. However, grating based approach requires precise control of grating parameters for efficient coupling and usually have low tolerance to wavelength variations. Unlike grating couplers[13,14], 45-degree surface-normal micro-couplers are easy to fabricate, reproducible and relatively insensitive to wavelength variations. Here, we describe the integration of 45-degree micro-couplers into H-tree waveguide structure.

2.1 Two-dimensional 45-degree Surface-normal Micro-coupler Array Fabrication

2.1.1 Fabrication using Reactive Ion Etching (RIE) Technique

The initial fabrication and characterization of polyimide waveguide mirror-coupler was done using RIE technique. A channel waveguides on a silicon wafer with 2μm thick silicon dioxide was fabricated using photolithography. We used RIE to fabricate the 45-degree micro-coupler at the end of each branch of the waveguide. The processing steps are shown in Fig. 5. A 0.3nm-thick aluminum film was coated over the waveguides followed by a photoresist (AZ5206E) layer. A mask was used to pattern the end portions of the waveguides. The pattern is then transferred to aluminum layer by wet etching. This opens a square window at each end of the waveguide. Aluminum layer acts as a mask in reactive-ion etching(RIE) chamber. The sample was mounted at 45 degree with respect to the electrode plates of the RIE chamber. A Faraday cage[15] was used to cover the sample so that the directional high-speed ions can attack the polyimide at 45 degree. After RIE process the aluminum mask was removed by aluminum etchant, leaving a 45-degree slanted end surface on each end of the waveguide. This 45-degree slanted end surface serves as the micro-coupler. The SEM micrograph of the cross section of a 45-degree micro-coupler is shown in Fig. 6 and a photograph showing waveguide mirror-coupler acting as a input-coupler is shown in the Fig. 7.

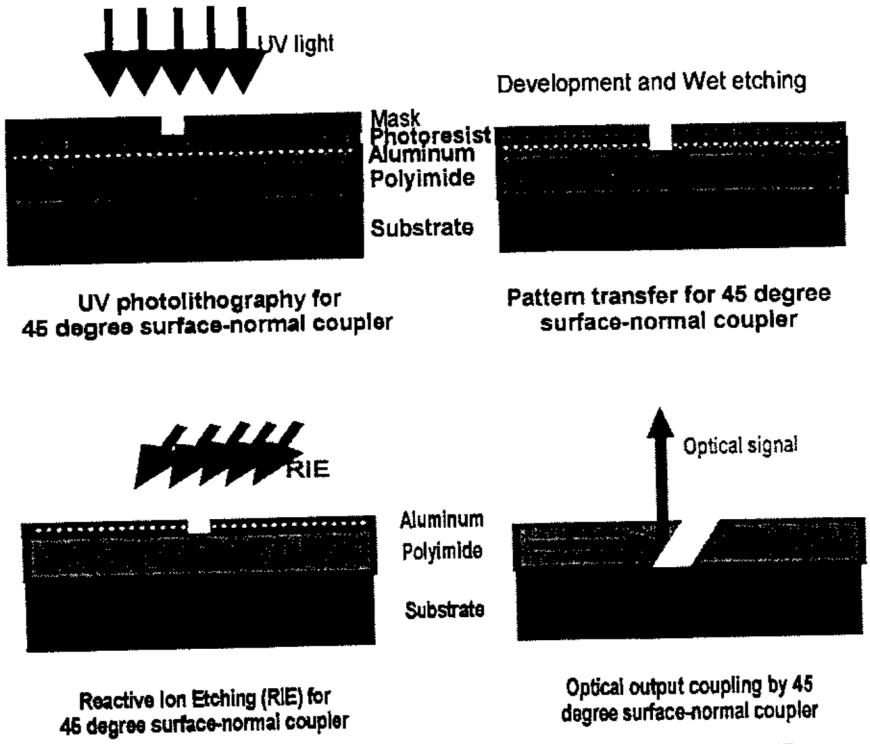

Fig. 5. The processing steps of making 45 degree micro-coupler using RIE

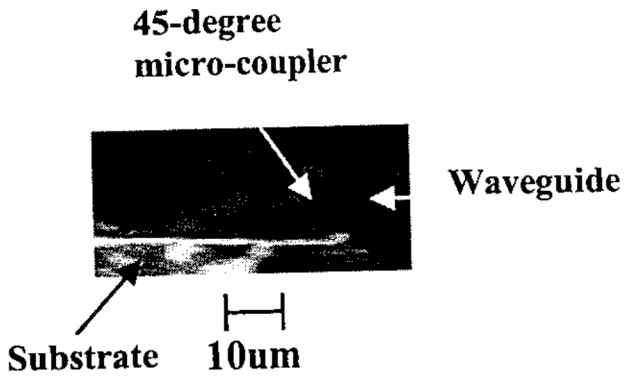

Fig. 6. The SEM micrograph of the cross section of the 45-degree micro-coupler at the end of waveguide

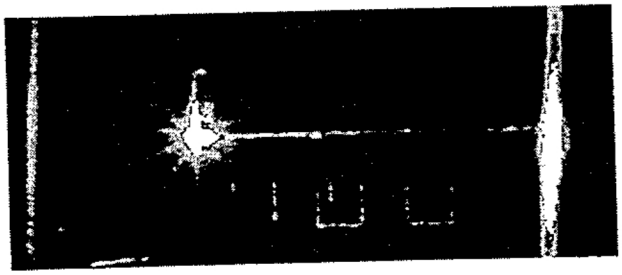

Fig. 7. A planar polyimide waveguide with waveguide mirror

2.1.2 Fabrication using Double exposure Technique

Because of limited size of the RIE chamber the reactive ion etching technique could not be applied to the large samples. To over come this problem, have also developed an alternative approach to fabricate the H-tree waveguide and 45-degree surface-normal micro-coupler using double exposure method. In double exposure method, the H-tree mask is placed over the sample and the lines of the H-tree mask are blocked using an additional "mask-1" (see fig. 8) which was slightly short at the end portions of the 48 branches and exposed to 45-degree-slanted UV light. Then we block the end portions of the 48 branches using another "mask-2" and let the line portions of the H-tree waveguides expose to normal-incident UV light. The patterned waveguides were processed using standard polyimide development procedure leaving stable and moisture-resistant polyimide waveguides with 45-degree slanted ends after final bake.

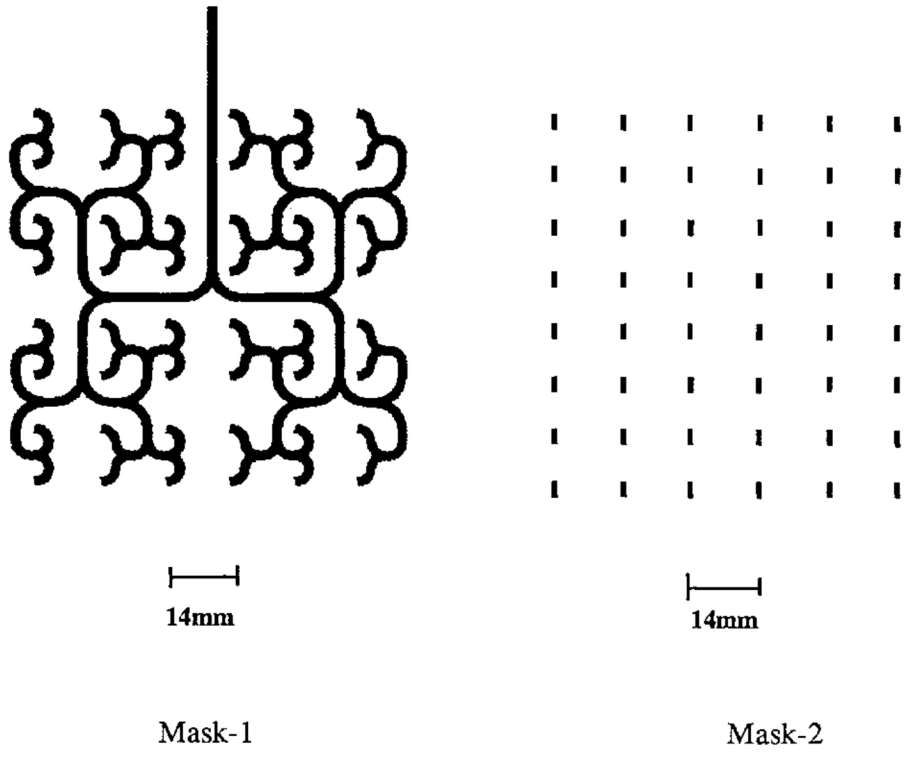

Fig. 8. "Mask-1" used to block the line portions of the waveguides during first 45-degree-slanted exposure, and "Mask-2" used to block the end portions of waveguides during second exposure

2.2 Measurement and Theoretical Simulation

To demonstrate the functionality of mirror couplers, butt coupling was used to couple the light into the waveguide. The surface-normal outputs from 48 output micro-couplers can be seen in Fig.9. However, the waveguide is also visible due to the high scattering loss at 633nm wavelength. The 48 surface-normal outputs from the 45-degree micro-couplers are shown. The waveguide loss is much lower when we use 850nm wavelength. The output wavelength of VCSEL is 850nm and the surface-emitting characteristic of VCSEL is a natural match to 45-degree surface-normal micro-coupler.

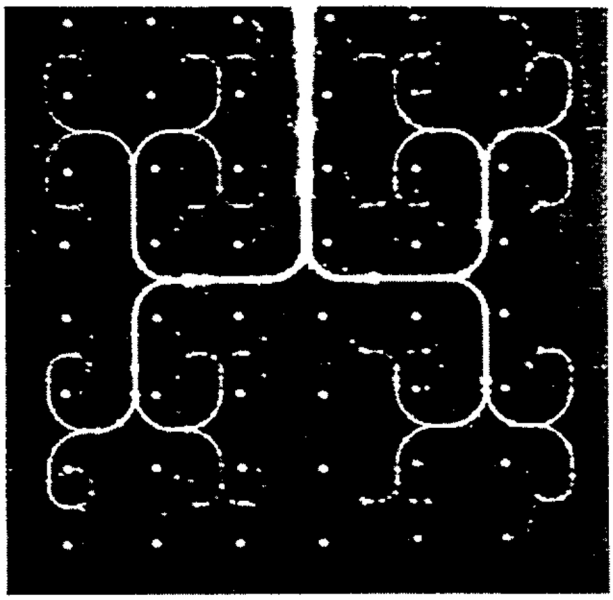

Fig. 9. A photography showing the 48 surface-normal outputs

The output profiles from one of the 45-degree micro-couplers are shown in Fig.10(a), (b) and (c). These figures correspond to z=100μm, z=1mm and z=5mm, respectively, where z is the distance from upper surface of the coupler to the point of observation. The output coupling efficiency of this 45-degree micro-coupler is nearly 100%. The half width at half maximum (HWHM) of the output profile at the micro-coupler is about 60μm, which is comparable with the active region of silicon-based photo detector having a bandwidth of 6GHz[16]. If the photodetectors are mounted close to the micro-couplers, then most of the light can reach the photo detectors and thus the coupler-to-detector coupling efficiency can be very high.

The output profile from the 45-degree micro-coupler can be determined using diffraction theory. According to Fresnel approximation[17], the near field distribution U(x, y) is given by:

$$U(x,y) = \frac{\exp(jkz)}{jz\lambda}\int_{-\infty}^{\infty} U(\xi,\eta)\exp\{(j\frac{k}{2z}[(x-\xi)^2+(y-\eta)^2]\}d\xi d\eta$$

Where $U(\xi,\eta)$ is the complex amplitude of the excitation at point (ξ,η) on the 45-degree micro-coupler, $U(x,y)$ the complex amplitude of the observed field at point (x,y), k the magnitude of wave vector and z the distance from the upper surface of the 45-degree micro-coupler to the point of observation. However, direct integration based on Fresnel approximation fails for a small z due to the fast oscillations of the Fresnel factor[18]. Modified convolution approach[18] was used to calculate the $U(x,y)$ and output profiles. The theoretical output profiles at z=100μm, z=1mm and z=5mm from the 45-degree micro-coupler are shown in Fig. 10(a'), (b') and (c'), respectively. In these calculations, the input to the micro-coupler was assumed to be the fundamental mode of the waveguide. This is a reasonable assumption since the most of the energy in a multimode waveguide remains confined to the fundamental propagating mode. Note that the input is in TEM_{00} mode. Compared to Fig. 10(c'), the side-lobes in Fig. 10(c) are not clear due to the poor contrast of the image. As z becomes larger, the output light diverges faster in the direction that corresponds to the smaller dimension of the 45-degree micro-coupler. There is a good agreement between the theoretically simulated and experimentally observed output profiles.

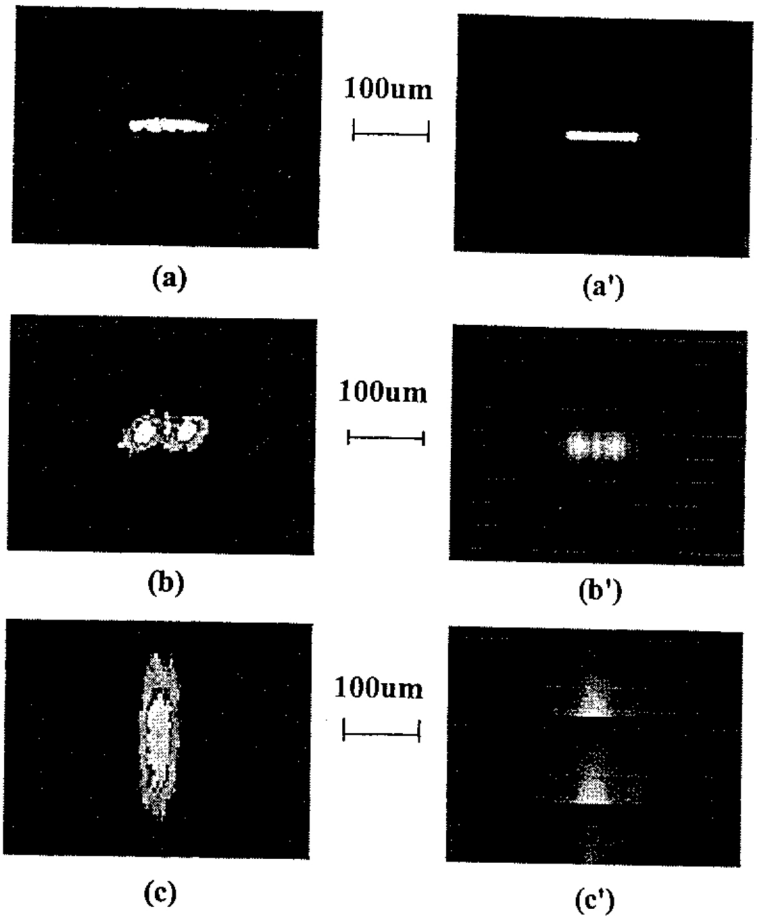

Fig. 10. The output profiles from the 45-degree surface-normal micro-coupler (a)z=100μm (experiment); (b)z=1mm (experiment); (c) z=5mm (experiment) (a')z=100 μm (theory); (b')z=1mm (theory); (c') z=5mm (theory)

3. POWER BUDGET EVALUATION

High-speed operation and massive fanout requirements impose stringent conditions on the material selection, minimization of waveguide propagation loss, and optimization of output coupling efficiencies. Ensuring that enough optical power reaches the photodetectors is essential for high-speed operation. For example, the total optical splitting power budget is 18 dB (3x6) in an optical H-tree system (capable of providing 64 fanouts), which consists of six stages of 1-to-2 (3 dB) optical fanout. If the optical power at the input end is 10 dBm, and a 10 GHz optical receiver (having a sensitivity of -20 dBm at 10 GHz)[19] is used at the output end for signal detection, the total insertion loss (output coupling loss plus waveguide propagation loss) should be less than 12 dB.

In the H-tree designed, the total length from base of first splitter to the fanout end is 10.4 cm. The measured propagation losses are 0.21 dB/cm at 850 nm and 0.58 dB/cm at 633 nm. This results in a total propagation loss of 2.18 dB at 850 nm and 6.03 dB at 633 nm. The splitting and bending loss for 6 stages is measured at 2.4 dB. (6 * 0.4 dB). Assuming a 3 dB input coupling loss and 90% output coupling efficiency, we project a total insertion loss of 7.98 dB at 850 nm and 11.83 dB at 633nm which is less than the maximum acceptable insertion loss of 12 dB.

4. SUMMARY

In summary, a polymer-based waveguides for optoelectronic interconnects and packaging has been fabricated and characterized. The fabrication process is compatible with Si-CMOS packaging process. An optoelectronic interconnection

layer (OIL) for the high-speed massive clock signal distribution for the Cray T-90 supercomputer board has been constructed. The optical interconnection layer under development employs optical multimode channel waveguides in conjunction with surface-normal waveguide mirror couplers and the 1-to-2 (3 dB) splitters. Equalized optical paths are realized using an optical H-tree structure having 48 optical fanouts. This device could be increased to 64 without introducing any additional complication. The 45-degree micro-couplers in guided-wave optical clock distribution system have been investigated. Both RIE and double exposure method were used to fabricate the 45-degree micro-couplers. The mirror-couplers have been integrated to 1-to-48 H-tree waveguide outputs and surface-normal output coupling is demonstrated. The output coupling efficiency is nearly 100%. If the photo detectors are mounted close to the micro-couplers, most of the light can reach the photo detectors having a distance of several microns and thus very high coupler-to-detector coupling efficiency is achievable. The final planarization step involving top cladding layer and the integration of VCSEL and photo detectors with H-tree waveguide and 45-degree micro-couplers are in progress. The high efficiency of surface-normal coupling is an obvious advantage when the optical clock distribution system is integrated with lasers and photo detectors for intra-chip, inter-chip and inter-board interconnects. The propagation loss and splitting loss have been measured as 0.21 dB/cm and 0.4 dB/splitter at 850 nm. The projected power budget is within acceptable range.

AKNOWLEDGEMENTS

This research is sponsored by DARPA, BMDO, AFOSR, Cray Research, 3M Foundation, Texas ATP program and OIDA Joint US-Japan Optoelectronics Project.

REFERENCES

1. J.W.Goodman, F.I.Leonberger, S.Y.Kung, and R.A.Athale, "Optical interconnections for VLSI systems", Proc. IEEE, Vol. 72, pp. 850-866, 1984.
2. M.R.Feldman, S.C.Esener, C.C.Guest, and S.H.Lee, "Comparison between optical and electrical interconnects based on power and speed considerations", Appl. Opt., Vol. 27, pp. 1742-1751, 1988.
3. Founad E. Kiamilev, Philippe Marchand, Ashok V. Krishnamoorthy, Sadik C. Esener, and Sing H. Lee, "Performance comparison between optoelectronic and VLSI multistage interconnects networks", IEEE J. of Light. Technol., Vol. 9, pp. 1674-1692, 1993.
4. Paola Cinato, Kenneth C. Young, Jr., "Optical interconnections within multichip modules", Opt. Eng., Vol. 32, pp. 852-860, 1993.
5. Bradley D. Clymer and Joseph W. Goodman, "Optical clock distribution to silicon chips", Opt. Eng., Vol. 25, pp. 1103-1108, 1986.
6. Suning Tang, Ray T. Chen and Mark Peskin, "Packing density and interconnection length of a highly parallel optical interconnect using polymer-based single-mode bus arrays", Opt. Eng., Vol. 33, pp. 1581-1586, 1994.
7. Ray. T. Chen, Suning Tang, T. Jannson and J. Jannson, "A 45 cm long compression molded polymer-based optical bus", Appl. Phys. Lett., Vol. 63, pp. 1032-1034, 1993.
8. R.T.Chen, "Polymer-based Photonic Integrated Ciucuits", (Invited Review Paper), Optics and Laser Technology, Vol. 25, pp. 347-365, 1993.
9. Ray. T. Chen, H. Lu, D. Robinson, Michael Wang, Gajendra Savant, and Tomasz Jannson, "Guided-wave planar optical interconnects using highly multiplexed polymer waveguide holograms", IEEE J. Light. Technol., Vol. 10, pp. 888-897, 1992.
10. M. R. Feldman, S. C. Esener, C.C. Guest, and S. H. Lee, "Comparison between optical and electrical interconnects based on power and speed considerations," Appl. Opt., vol. 27, pp. 1742-1751, 1988.
11. Feiming Li, Linghui Wu, Bipin Bihari, Suning Tang and Ray T. Chen," Unidirectional surface-normal wave-guide grating couplers for wafer-scale MCM interconnect," to be submitted to IEEE Photonics Tech. Lett.
12. G.J. Velduis and P.V. Lambeck, "highly-sensitive integrated optical spiral-shaped waveguide refractormeter", Appl. Phys. Lett, 71(20), 17 November 1997
13. R. Waldhausl, B. Schnabel, P. Dannberg, E. Kley, A. Brauer, and W. Karthe, Applied Optics, Vol. 36, 9383(1997).

14. J. Miller, N. de Beaucoudrey, P. Chavel, J. Turunen, and E. Cambril, Applied Optics, Vol. 36, 5717(1997).
15. G. D. Boyd, L. A. Coldren, F. G. Storz, Applied Physics Letter, Vol. 36, No.7, pp. 583-585, 1980.
16. J. C. Campbell, Photodetectors for Optoelectronic Integrated Circuits, in Integrated Optoelectronics, edited by M. Dagenais, R. F. Leheny, and J. Crow, Academic Press, Chapter 11, 424(1995).
17. J. W. Goodman, Fourier optics, McGraw-Hill Publishers, second edition, New York, Chapter 4, pp.63-89, 1996.
18. M. Sypek, Optics Communications, Vol. 116, 43-48(1995).
19. Data Sheet of G4176-020, Hamamatsu Photonics K.K